Structural Transformation of $LiFePO_4$ During Ultrafast Delithiation

Christian Kuss,[a†] *Ngoc Duc Trinh,*[a] *Stefan Andjelic,*[a] *Mathieu Saulnier,*[a] *Eric M. Dufresne,*[b]

Guoxian Liang[c] *and Steen B. Schougaard*[a]**.*

AUTHOR ADDRESS

[a] Université du Québec à Montréal, Département de chimie, C.P. 8888, Succ. Centre-ville, Montreal (QC), Canada H3C 3P8.

[b] Argonne National Laboratory, Advanced Photon Source, 9700 South Cass Ave, Argonne IL 60439, USA.

[c] Johnson Matthey Battery Materials Ltd, 280 ave Liberté, Candiac (QC), Canada J5R 6X1.

AUTHOR INFORMATION

† Present Affiliation: University of Oxford, Department of Materials, Parks Road, Oxford, UK OX1 3PH.

Corresponding Author

*schougaard.steen@uqam.ca.

ABSTRACT

The prolific lithium battery electrode material lithium iron phosphate ($LiFePO_4$) stores and releases lithium ions by undergoing a crystallographic phase change. Nevertheless, it performs unexpectedly well at high rate and exhibits good cycling stability. We investigate here the ultrafast charging reaction to resolve the underlying mechanism, while avoiding the limitations of prevailing electrochemical methods by using a gaseous oxidant to deintercalate lithium from the $LiFePO_4$ structure. Oxidizing $LiFePO_4$ with nitrogen dioxide gas reveals structural changes through *in situ* synchrotron X-ray diffraction and electronic changes through *in situ* UV/Vis reflectance spectroscopy. This study clearly shows that ultra-high rates reaching 100% state of charge in 10s, does not lead to a particle-wide union of the *olivine* and *heterosite* structures. An extensive solid solution phase is therefore *not* a prerequisite for ultra-fast charge/discharge.

.

TOC GRAPHIC

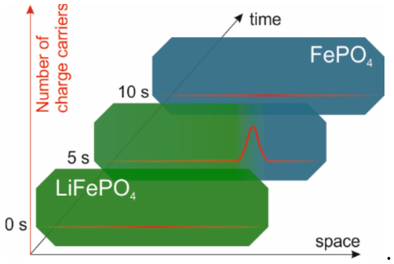

KEYWORDS *In-Situ*, structural analysis, electronic structure, biphasic, XRD, Uv-vis, reaction mechanism, lithium-ion.

Improving charging rates is a major challenge in renewable electrical energy storage. *E.g.* consumers would be more accepting of a 200 km electric car driving range, if recharging required only minutes rather than hours. Focusing on the lithium-ion technology due to its high energy density, the charging rate is ultimately determined by the constituent materials. Among these, lithium iron phosphate $LiFePO_4$ is a safe, environmentally benign, economical and competitively performing positive electrode material.[1] During charging and discharging, intermediate compositions Li_xFePO_4 $(1<x<0)$ are created, which, under equilibrium conditions, phase separate to *heterosite* $Li_{0.04}FePO_4$ and *olivine* $Li_{0.96}FePO_4$.[2] This phase separation diminishes the number of electronic and ionic transport species, and thus, in theory, the reaction rate. Yet, $LiFePO_4$ has been shown to achieve remarkably fast extraction and insertion of lithium[3-5]. The microscopic origin of this paradox is still a subject of intense debate. Thermodynamic considerations predict that high driving forces can transiently remove lithium beyond the thermodynamic solid solution limits, at which the slope and curvature of the free energy curve determine how far the composition can deviate from the thermodynamic limits. Theoretical attempts to make that quantification suggest the formation of a full solid solution at high overpotential.[6] In an *in situ* X-ray diffraction study, Liu and co-workers have confirmed that metastable lithium concentrations in Li_xFePO_4 can be achieved when charging at a 10C rate.[7] The ensuing inference that a macroscopic lithium solid solution is a prerequisite for ultra-high rate performance will be tested here.

Beyond $LiFePO_4$, elucidating the ultra-high rate mechanism is of high technological interest. The energy density is limited by the comparably low potential of the $Fe^{+2/+3}$ couple (3.4V vs. Li/Li^+), rendering it unsuited in many applications. Great expectations have therefore been placed on the isostructural $LiMnPO_4$ and similar *olivine* transition metal lithium phosphates which exhibit improved redox potentials. These, however, have found very limited application as they do not exhibit $LiFePO_4$ remarkable charge/discharge rate.[8] *If* phase separation in $LiFePO_4$ persists at ultra-high rate, the mere presence of a two-phase system in these *olivines* cannot be the cause of their kinetic limitations.

One of the major challenges of high rate measurements is that high current densities are required to pass through the electrode. Within common composite electrodes, this leads to significant polarization, both electronically within the electronic conduction path, and ionically within the electrolyte. Consequently, the electrode exhibits significant spatial variation in reaction conditions.[9] Alternatively, single particle techniques limit drastically the sample volume, which, combined with the required time resolution, leads to poor signal-to-noise ratios.[10] Thus, the recently discovered high rate delithiation reaction of $LiFePO_4$ with the gaseous oxidant NO_2, whose reaction free energy corresponds to a charge at about 4.1 V *vs.* Li/Li^+, provides a rare opportunity to study ultra-fast delithiation.[4] Importantly, it can be combined with visible and X-ray light sources to obtain high time-resolution *in situ* X-ray diffraction and electronic spectra, since carbon coating of the metal phosphate is not required.

Here, we use this gas-solid reaction to drive *complete* lithium extraction to the highest reported speed at ambient conditions, and simultaneously follow structural and electronic changes with high time resolution using *in situ* synchrotron X-ray diffraction and optical reflectance spectroscopy. We show that even in this ultrafast limit, phase separation competes successfully with the kinetically accessed solid solution mechanism.

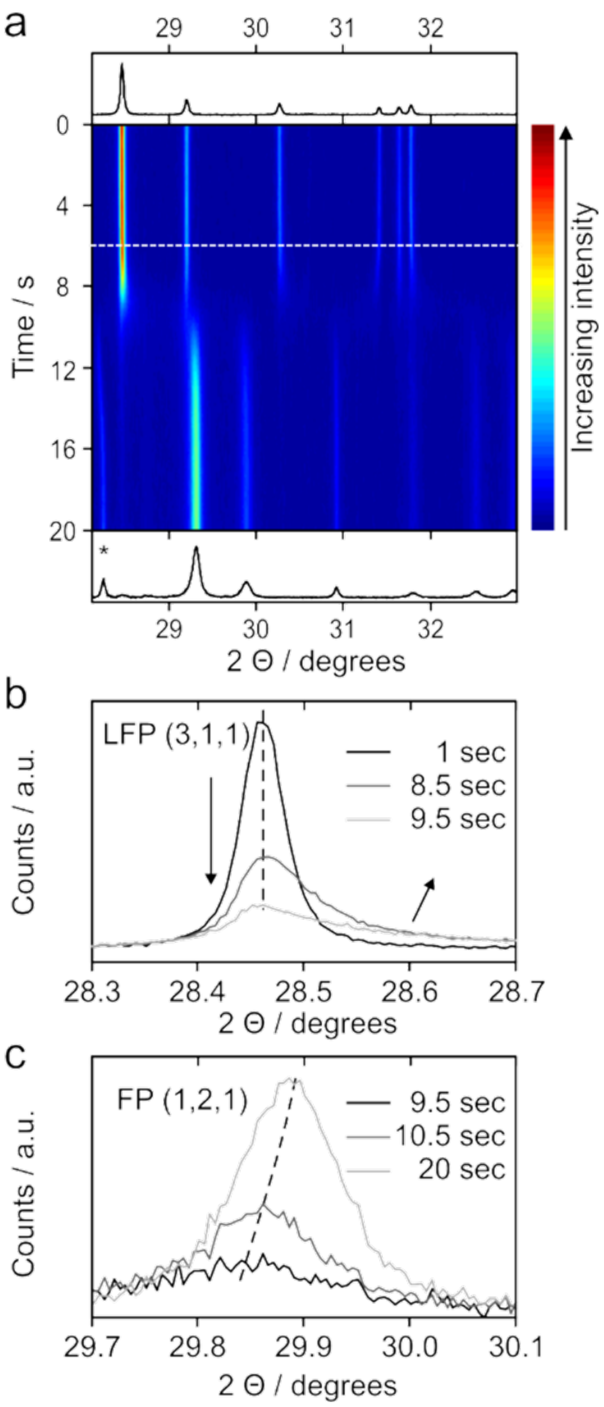

Figure 1. *Time dependent diffraction during complete oxidation. a. Diffraction intensity vs. diffraction angle-time contour map (X-ray energy 10 keV, wavelength 1.24 Å). The top line plot shows the initial, the bottom line plot the final diffractogram (asterisks mark reflections of the* $LiNO_3$ *phase). Gas injection was started at 2 seconds, and was measured to arrive at the sample*

at 6 ± 1 seconds (white dashed line). b. $LiFePO_4$ (3,1,1) reflections during the phase transition (increasing time is displayed in lighter grey). The reflections intensity decreases and the peak width increases asymmetrically. (black arrows) Whereas the peak maximum remains largely unmoved (dashed line), the peak center shifts to higher angles. C. $FePO_4$ (1,2,1) reflection during phase transition. As the reflection grows the peak maximum shifts to higher angles (dashed line), whereas no significant peak asymmetry is observed.

The full delithiation of $LiFePO_4$ with NO_2 gas is shown in a time-diffractogram map in Figure 1a. NO_2 flow is started at time = 2 seconds, and the flow has been measured to arrive at the powder at about 6 seconds. At 16 seconds, *i.e.* only 10 seconds after the arrival of the gas, the material has been completely transformed to the lithium poor phase. The deintercalation of lithium during this structural rearrangement is further confirmed by the concurrent formation of crystalline $LiNO_3$. At well below 20 seconds, this complete transformation from $LiFePO_4$ to $FePO_4$ has never been observed at such speeds *in situ*. This high rate, made possible by the NO_2 gas phase reaction, is especially noteworthy considering that commercial $LiFePO_4$ particles with diameters greater than 200 nm were used here.

Given this fast rate, it is very likely that the reaction is mainly limited by lithium transport. During the 10 second transformation reaction, the initial single-phase modification within the lithium rich structure can be observed in the first 2 to 3 seconds. Subsequently, the lithium rich and lithium poor phase both exhibit considerable diffraction intensity during a period of at least 2 seconds, indicating co-existence of both phases within particles.

Investigating the diffractograms of both phases individually, the lithium rich phase diffraction peaks widen with significant asymmetry as their intensity diminishes and pronounced micro-strains are formed (Figure 1b). Accordingly, the peak width has been quantified to increase to about three-fold the initial value. While a significant volume of the lithium rich phase must be strained to lead to such well-visible peak asymmetry, the diffraction angle of the lithium rich phase peak maxima remains largely unchanged. As such, throughout the delithiation process, most of the remaining lithium rich phase waits in its pristine structure and strong micro-strains appear only locally. In contrast, the lithium poor phase bulk structure contracts as it crystallizes, as witnessed by the moving peak maxima (Figure 1c). The peak width reduces significantly during the phase transformation, but does not reach the value of the $LiFePO_4$ starting material, suggesting smaller crystallite size, residual symmetric strains or defects in this phase. The peak width of the starting $LiFePO_4$ sample is, within Scherrer's approximation, consistent with the average particle size of about 200 nm. From the peak width of the product, a reduction of the coherently scattering domain length to about 80 nm can be determined. Similarly, qualitative assessment of the diffraction data suggests a temporary decrease in total diffraction intensity during the phase transformation. The inferred formation of a low-crystallinity intermediate phase cannot be excluded. Thus, qualitatively the lithium poor structure crystallizes homogenously with imperfections, whereas the lithium rich structure responds to its oxidation with pronounced local micro-strains.

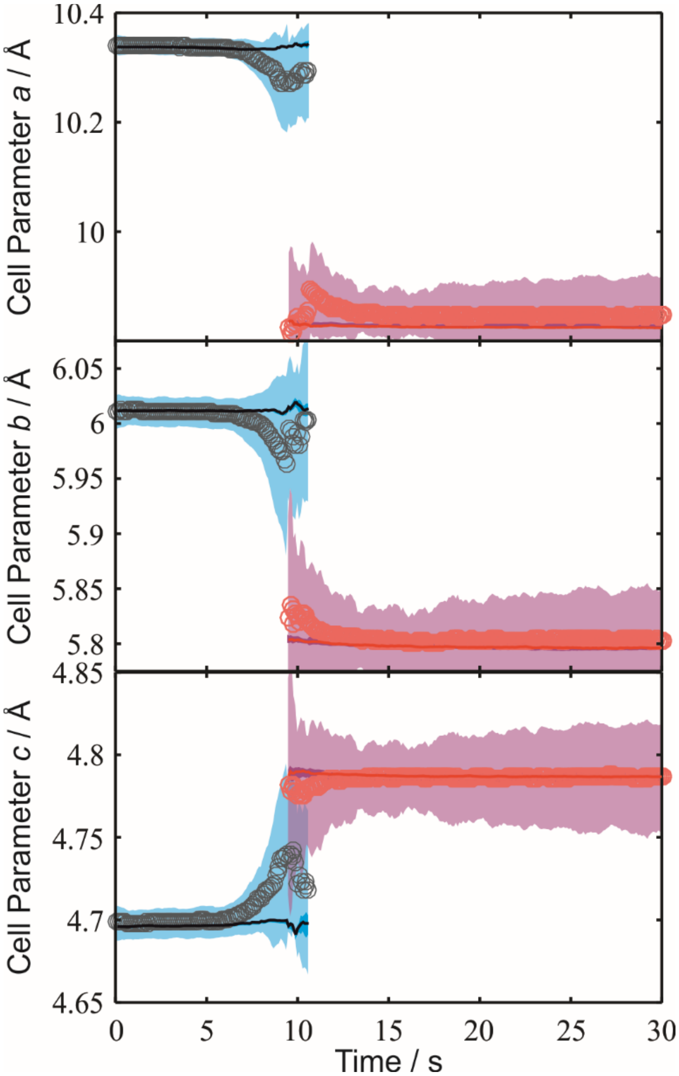

Figure 2. *Structure refinement. Cell parameters of the bulk structure (lines), and the average structure (circles) of the lithium rich (black/grey) and lithium poor (red/pink) phase. Confidence intervals for these parameters are shown as light shaded areas for the average cell parameters, and as dark shaded areas for the maximum cell parameters.*

In order to obtain bulk structural parameters and to quantify the observed strain, we fitted calculated diffractograms to the recorded patterns, allowing for the refinement of a bulk structure, representing the diffraction peak maxima, and an average structure, representing the diffraction peak means, thus accounting for peak asymmetry (details in the Supporting Information) and providing a quantification of the asymmetric strain. Figure 2 shows strongly strained average structures, well beyond the thermodynamically stable compositional strain. Applying Vegard's law, approximate average compositions down to $Li_{0.75}FePO_4$ and up to $Li_{0.15}FePO_4$ can be found. However, even the strongly strained *a* and *b* axes still exhibit an abrupt change of average lattice parameters from one phase to the other. Further, no diffraction intensity is observable between the (4,1,0) reflections of the lithium rich and poor phases (Figure 3). While this cannot be evidence to exclude transient completely disordered states, that do not show coherent diffraction, or small disordered zones at the interface,[11] it nevertheless dispels continuous solid solution between $LiFePO_4$ and $FePO_4$ with dimensions comparable to the particles.

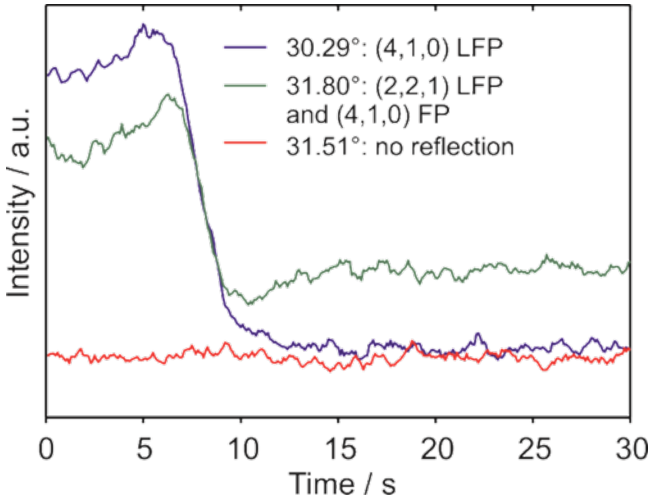

Figure 3. *Diffraction intensity of the (4,1,0) reflections of $LiFePO_4$ (LFP, 30.29°) and $FePO_4$ (FP, 31.80°) and the background in between the two peaks (31.51°). A continuous solid solution between both phases would entail an increase in the diffraction intensity of the background between the two peaks.*

The origin of the observed inhomogeneous strain of the lithium rich phase may be a compositional change, *i.e.* lithium concentration gradients, or formation of a coherent interface, which leads to coherency strain. Following Vegard's law, compositional strain would be isotropic, while coherency strain exhibits anisotropy, depending on the crystallographic orientation of the interface. The absence of significant anisotropy in the normalized strain favours inhomogeneous lithium concentrations in the Li_xFePO_4 structure rather than interface coherency as being responsible for the peak asymmetry.

Similar to these findings, the work by Liu *et al.*[7] shows a distribution of lattice parameters during the phase transition. However, the width of this lattice parameter distribution is wider then we observe. Moreover, the published rate dependency suggests an increase in solid solution phase with increasing rate. Yet, we observe a narrower cell parameter distribution while delithiating at a rate at least 18 times greater. The origin of this discrepancy may be explained by the increasing inhomogeneity within the composite electrode in the electrochemical experiment. As a composite electrode exhibits an internal electronic and ionic resistance, an increasing rate leads to higher inhomogeneity among the probed delithiating $LiFePO_4$ particles, which naturally increases the width of the lattice parameter distribution. Conversely, the gas delithiation experiment exposes the whole sample to a homogeneous concentration of oxidant. Thus[CKD1], the presented structural data present a picture of a meta-stable wide distribution of lithium concentrations, that remains strongly inhomogeneous over the whole particle population, as phase separation competes with the dynamic delithiation even at the presented ultra-high rates.

The proposed localized lithium concentration gradient would entail iron mixed valence, and thus a spectral signature. Making use of the particle size dependence of the stable solid solution ranges within Li_xFePO_4, Yamada *et al.* showed that mixed valence in Li_xFePO_4 leads to a strong intervalence charge transfer band in the visible light absorption spectrum (shaded region in Figure 4a).[12] This transfer band has not previously been studied during dynamic delithiation, since the carbon coating required for electrochemical oxidation precludes its observation. During the chemical oxidation of *uncoated* $LiFePO_4$ (Figure 4b) a strong transient decrease in reflectance in the 600-900 nm region is observed, confirming the transient presence of mixed valence. Moreover, the appearance of this feature correlates closely with the increase of diffraction intensity in a mixed valence region (30.46° 2 θ, corresponding to the strained (4,1,0) plane) of this slower reacting carbon-free sample (Figure 4d). The spectroscopic analysis therefore confirms that the observed diffraction peak asymmetry is an effect of interface region with inhomogeneous lithium concentration and mixed valence on the iron site.

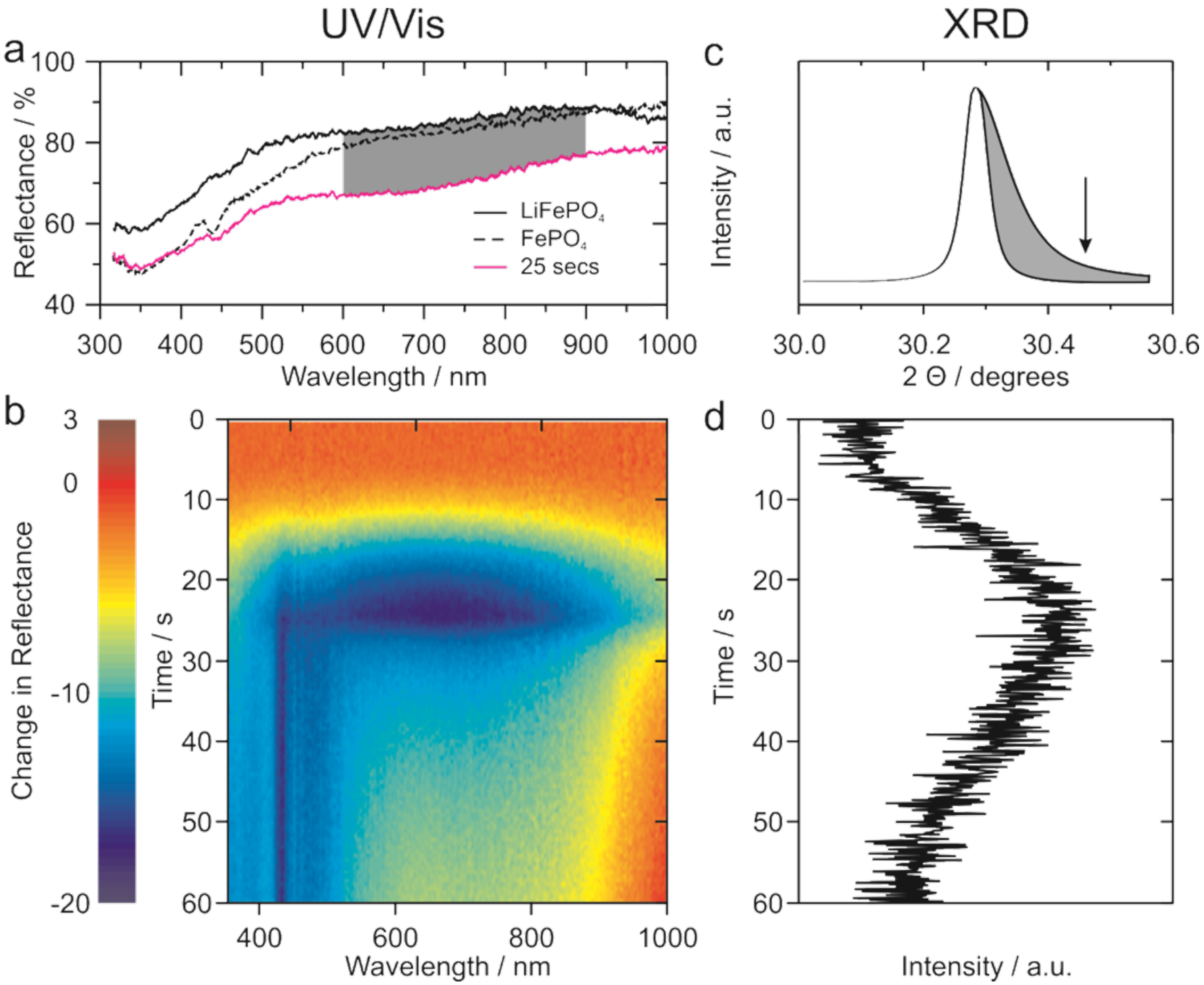

Figure 4. *Evidence of the transient mixed valence correlated to interfacial strain. a. Reflectance spectra of pristine* $LiFePO_4$*,* $LiFePO_4$ *after 25 seconds of* NO_2 *gas exposure, and* $FePO_4$ *showing a significant transient decrease in reflectance in the mixed valence region (shaded). b. Change in reflectance (%) from initial spectrum showing transient decrease in reflectance in the mixed valence region from 600 to 900 nm and permanent changes due to the phase change and absorption by the* NO_2 *gas in the region up to 600 nm. c. Fitted (4,1,0) reflection of lithium rich phase during phase transition, showing significant asymmetry, which accounts for composition strain. The arrow marks the angle chosen for the intensity plot in d. d. Transient increase in diffraction intensity at 30.46 ° (asymmetry region of (4,1,0) reflection of the lithium rich phase).*

The concentration increase of both ionic and electronic charge carriers that ensues the extended compositional range of the mixed valance state is required for the ultra-high delithiation reaction rate witnessed here. Yet, the concurrent phase separation suggests that the observed lithium solid solution exhibits a transitional maximum in free energy. The energy barrier for phase transition between the crystallographically distinct lithium rich and lithium poor phases would however be strongly modified by the smaller unit cell mismatch arising from the formation of the concentration gradient. In accordance, no build-up of the strained structure diffraction peaks, as the bulk $LiFePO_4$ peak is disappearing, can be found. Consequently, the conversion from the strained lithium rich to the crystallographically distinct lithium poor phase is not rate limiting.

With the presented methodology, it is possible to probe the atomic and electronic structure of $LiFePO_4$ at rates far beyond the abilities of current batteries. Moreover, this is achieved while continuously exposing the material to a homogenous driving force. Passing to sub-minute charging rates would be an exceptional success in the development of intercalation material based batteries, and arguably satisfy even the highest fast-charge requirements. The present work shows that this is achievable in two-phase intercalation materials, even when phase separation macroscopically persists. Microscopic access to a widened solid solution along the interface between the two limiting phases can be sufficient to create enough charge carriers for charging rates at the ten-second time scale.

Experimental Methods

General information. Carbon coated and carbon free $LiFePO_4$ with average particle sizes larger than 200 nm was obtained from Johnson Matthey Battery Materials. NO_2 was purchased from Air Liquide. Delithiations were performed in a temperature controlled stainless steel cell with polyimide x-ray window. Diffractograms were recorded in reflection with 10 keV X-rays and a Dectris area detector at a 10 Hz rate. X-ray diffraction experiments were performed at the 7-ID beamline of the Advanced Photon Source. A boxcar filter over 6 diffractograms was applied in the time axis. Gas flow was controlled at 20 ml/min with syringe pumps. Diffractograms were fitted using a scripted fitting routine in Matlab. Details of this procedure can be found in the supporting information. UV/Vis spectra were also recorded in diffuse reflectance in the same stainless steel cell with a glass window. Experiments are explained in more detail in the supporting information.

Hazards. Oxidizing gases that are suited for delithiation of $LiFePO_4$, e.g. NO_2 or Cl_2, are highly corrosive and toxic. All such experiments should be performed in a self-contained system.

Supporting Information. Detailed experimental information and diffraction pattern fitting procedure.

Notes

Johnson Matthey Battery Materials Ltd, is a producer of c-$LiFePO_4$.

ACKNOWLEDGMENT

This work received financial support through the Natural Sciences and Engineering Research Council of Canada (NSERC), Grant CRD 385812-09. Use of the Advanced Photon Source, an Office of Science User Facility operated for the U.S. Department of Energy (DOE) Office of Science by Argonne National Laboratory, was supported by the U.S. DOE under Contract No. DE-AC02-06CH11357.

REFERENCES

1. Padhi, A. K.; Nanjundaswamy, K. S.; Goodenough, J. B. Phospho-olivines as Positive-Electrode Materials for Rechargeable Lithium Batteries. J. Electrochem. Soc. 1997, 144 (4), 1188-1194.
2. Yamada, A.; Koizumi, H.; Sonoyama, N.; Kanno, R. Phase Change in Li_xFePO_4. Electrochem. Solid-State Lett. 2005, 8 (8), A409-A413.
3. Huang, Y.-H.; Wang, F.-M.; Huang, T.-T.; Chen, J.-M.; Hwang, B.-J.; Rick, J. Micro-Electrode Linked Cyclic Voltammetry Study Reveals Ultra-Fast Discharge and High Ionic Transfer Behavior of $LiFePO_4$. Int. J. Electrochem. Sci 2012, 7, 1205-1213.
4. Kuss, C.; Lepage, D.; Liang, G.; Schougaard, S. B. Ultrafast charging of $LiFePO_4$ with gaseous oxidants under ambient conditions. Chemical Science 2013, 4 (11), 4223-4227.
5. Zaghib, K.; Dontigny, M.; Guerfi, A.; Trottier, J.; Hamel-Paquet, J.; Gariepy, V.; Galoutov, K.; Hovington, P.; Mauger, A.; Groult, H.; Julien, C. M. An improved high-power battery with increased thermal operating range: C–$LiFePO_4$//C–$Li_4Ti_5O_{12}$. J. Power Sources 2012, 216 (0), 192-200.
6. Bai, P.; Cogswell, D. A.; Bazant, M. Z. Suppression of Phase Separation in $LiFePO_4$ Nanoparticles During Battery Discharge. Nano Lett. 2011, 11 (11), 4890-4896.
7. Liu, H.; Strobridge, F. C.; Borkiewicz, O. J.; Wiaderek, K. M.; Chapman, K. W.; Chupas, P. J.; Grey, C. P. Capturing metastable structures during high-rate cycling of $LiFePO_4$ nanoparticle electrodes. Science 2014, 344 (6191).
8. Yonemura, M.; Yamada, A.; Takei, Y.; Sonoyama, N.; Kanno, R. Comparative Kinetic Study of Olivine Li_xMPO_4 (M = Fe , Mn). J. Electrochem. Soc. 2004, 151 (9), A1352-A1356.
9. Schougaard, S. B. A nanoview of battery operation. Science 2016, 353 (6299), 543-544.
10. Danis, L.; Gateman, S. M.; Kuss, C.; Schougaard, S. B.; Mauzeroll, J. Nanoscale Measurements of Lithium-Ion-Battery Materials using Scanning Probe Techniques. ChemElectroChem 2017, 4 (1), 6-19.
11. Niu, J.; Kushima, A.; Qian, X.; Qi, L.; Xiang, K.; Chiang, Y.-M.; Li, J. In Situ Observation of Random Solid Solution Zone in $LiFePO_4$ Electrode. Nano Lett. 2014, 14 (7), 4005-4010.

12. Furutsuki, S.; Chung, S.-C.; Nishimura, S.-i.; Kudo, Y.; Yamashita, K.; Yamada, A. Electrochromism of Li_xFePO_4 Induced by Intervalence Charge Transfer Transition. Journal of Physical Chemistry C 2012, 116 (29), 15259-15264.